Journal of Catalysis 283 (2011) 124–132

Contents lists available at SciVerse ScienceDirect

Journal of Catalysis

journal homepage: www.elsevier.com/locate/jcat

Electrochemical promotion of the water–gas shift reaction on Pt/YSZ

S. Souentie [a,*], L. Lizarraga [a], A. Kambolis [a], M. Alves-Fortunato [a], J.L. Valverde [b], P. Vernoux [a]

[a] Université de Lyon, Institut de Recherches sur la Catalyse et l'Environnement de Lyon, UMR 5256, CNRS, Université Claude Bernard Lyon 1, 2 Avenue A. Einstein, 69626 Villeurbanne, France
[b] Departamento de Ingeniería Química, Facultad de Ciencias Químicas, Universidad de Castilla-La Mancha, Avenida Camilo José Cela 10, 13005 Ciudad Real, Spain

ARTICLE INFO

Article history:
Received 18 May 2011
Revised 27 July 2011
Accepted 28 July 2011
Available online 7 September 2011

Keywords:
Water–gas shift
Electrochemical promotion
EPOC
NEMCA effect
Pt electrode
YSZ

ABSTRACT

The effect of electrochemical promotion of catalysis was investigated for the water–gas shift reaction over porous Pt catalyst electrodes interfaced with 8%mol Yttria-stabilized Zirconia. A fuel cell type electrochemical reactor was used at temperatures from 300 °C to 400 °C, under P_{H_2O}/P_{CO} ratio values from 2.85 to 31. A negative order dependence of the catalytic reaction rate on P_{CO} and a positive one on P_{H_2O} was found under open-circuit and polarization conditions. Positive potential application (+2.5 V), i.e., O^{2-} supply to the catalyst surface, causes a small decrease in the catalytic reaction rate, while negative potential application (−1.5 V) results in a pronounced rate increase, up to 200%, with apparent faradaic efficiency values up to 110. The rate increase obtained with negative polarization can be attributed to the weakening of the Pt–CO bond strength but also, to the increase in surface concentration of oxygen ion vacancies near the Pt-gas-support three-phase boundaries necessary for water dissociation.

1. Introduction

The technologies of hydrogen production and purification will be of great importance in the hydrogen-energy economy in the near future. In the water–gas shift (WGS) reaction Eq. (1), hydrogen is produced from water in the presence of CO. This reaction is a key technology in the hydrogen purification processes of syn-gases obtained by steam reforming or partial oxidation of hydrocarbons [1,2].

$$CO + H_2O \rightarrow CO_2 + H_2 \quad (1)$$

The WGS state-of-the-art industrial process occurs in two steps to overcome the thermodynamic limitations at higher temperatures (moderately exothermic reaction, $\Delta H^\circ = -41.1$ kJ/mol), including a high-temperature (350–500 °C) shift (HTS) utilizing a Fe_2O_3/Cr_2O_3 catalyst, followed by a low-temperature (200–250 °C) one (LTS) over a $Cu/ZnO/Al_2O_3$ catalyst [1]. However, a single-step WGS process would be more desirable, avoiding the technical complexities of a multistep process.

Supported noble metal (e.g., Pt, Pd and Au) catalysts are reported as promising single-step WGS catalysts, due to their high catalytic activity at low temperatures, tolerance in chemical poisoning (Cl and/or S), long-term stability at high temperatures and regenerative potential after deactivation as a result of prolonged use. Recently, a sulfur-resistant commercial WGS catalyst has been reported by de la Osa et al. [3] using an industrial coal-derived syn-gas feed at elevated temperatures (up to 500 °C) and pressures (19 bar).

The WGS pathway and the exact nature of any intermediates formed are still under discussion; however, it is generally agreed that both the metal and the support play essential roles. Among the two reactants, i.e., CO and H_2O, the latter is more difficult to be activated due to its thermodynamic stability [4]. It has been reported that Pt cannot activate water under WGS reaction conditions [5]. Thus, in Pt-based WGS catalysts, a hydrophilic oxide support is required to adsorb and activate water [4–9], while Pt can adsorb and activate CO.

In the case of Pt/CeO_2 catalysts, two main different reaction pathways have been proposed in literature [6,10]: (i) the associative [11–14] and (ii) the regenerative red–ox mechanism [5,7,15,16]. In the associative mechanism [11–14], terminal hydroxyl groups of the support react with CO on Pt to form surface formate intermediate (reaction (2)). The decomposition of the formate species is suggested to be facilitated by the presence of water and is proposed to be rate determining (reaction (3)). No oxygen is removed from the surface during the catalytic cycle, and the oxide does not undergo any red–ox changes during the WGS reaction sequence, since water activation occurs on the formed formate intermediates.

$$Pt - CO + OH_{sup} + H_{sup} \rightarrow Pt - [COOH] - s_{sup} + H_{sup} \quad (2)$$

$$Pt - [COOH] - s_{sup} + H_{sup} \overset{+H_2O}{\rightarrow} CO_2(g) + H_2(g) + OH_{sup} + H_{sup} + Pt \quad (3)$$

* Corresponding author.
E-mail address: souentie@chemeng.upatras.gr (S. Souentie).

0021-9517/$ - see front matter © 2011 Elsevier Inc. All rights reserved.
doi:10.1016/j.jcat.2011.07.009

In the regenerative red–ox mechanism [5,7,15,16], CO is adsorbed on the metal particles and reacts at the metal-gas-support three-phase boundaries (tpb) with the oxygen from the support, forming CO_2 and creating a surface oxygen vacancy, V_O (reaction (4)). The support is then re-oxidized by H_2O forming H_2 (reaction (5)).

$$Pt - CO + O_{sup} \rightarrow CO_2(g) + Pt + V_O \quad (4)$$

$$V_O + H_2O \rightarrow O_{sup} + H_2(g) \quad (5)$$

Recently, an "associative formate with red–ox regeneration" hydride mechanism has been proposed for the case of Pt/ZrO_2 [17,18]. In this mechanism, hydroxyl groups on the zirconia surface react with CO to form intermediate formate. The latter can decompose to H_2 and CO_2, leaving oxygen vacancies that are filled by hydroxyl groups (reactions (6) and (7)), causing red–ox changes to the support during the WGS reaction sequence.

$$Pt - CO + OH_{sup} \rightarrow Pt - [COOH] - s_{sup} \overset{H_{sup}}{\rightarrow} CO_2(g) + H_2(g) + Pt + V_O \quad (6)$$

$$V_O + H_2O \rightarrow H_{sup} + OH_{sup} \quad (7)$$

The exact role of Pt is still under discussion. Most groups [4–9,17] propose that CO is adsorbed on Pt and reacts at the Pt-gas-support tpb. However, Korhonen et al. [19] and Graf et al. [18] have recently demonstrated that Pt is not necessary for the formation of the formate intermediate, but for its afterward decomposition to CO_2 and H_2, which is on the other hand, the rate determining step of the associative mechanism.

The chemical promotion of the WGS catalysts by alkalis has been investigated in several studies [20–24]. A parallel approach to the classical chemical promotion is the use of electrochemical promotion of catalysis (EPOC or non-faradaic electrochemical modification of catalytic activity, NEMCA effect) to electrochemically promote metal catalyst electrodes deposited over solid electrolyte supports, e.g., YSZ, TiO_2 or CeO_2. Such an electrode can also be used as an electrochemical sensor. The idea of using a metal electrode simultaneously as a catalyst to measure potentiometrically the electrochemical potential, or thermodynamic activity, of oxygen on metal catalysts, and thus to study catalytic mechanisms, was originally proposed by Wagner [25] and led to the technique of solid electrolyte potentiometry (SEP).

The phenomenon of electrochemical promotion of catalysis has been extensively investigated in the last 30 years for more than 70 catalytic reaction systems [26,27]. In EPOC studies, the conductive catalyst electrode is in contact with an ionic conductor ceramic support, and the catalyst (e.g., noble metals and oxides) is electrochemically promoted by applying a current or overpotential between the catalyst film and a counter or reference electrode, respectively. The cell overpotential is defined as:

$$\eta = U - U_{oc} \quad (8)$$

where U is the applied potential difference and U_{oc} the open-circuit potential difference.

Numerous surface science and electrochemical techniques have shown that EPOC is due to electrochemically controlled migration (reverse spillover or backspillover) of promoting ionic species (O^{2-} in the case of YSZ, TiO_2 and CeO_2, Na^+ or K^+ in the case of β''-Al_2O_3, protons in the case of Nafion, CZI ($CaZr_{0.9}In_{0.1}O_{3-\alpha}$) and BCN18 ($Ba_{3}Ca_{1.18}Nb_{1.82}O_{9-\alpha}$), etc.) between the ionic or mixed ionic–electronic conductor-support and the gas exposed catalyst surface, through the catalyst-gas-electrolyte tpb. These backspillover species, accompanied by their compensating (screening) charge δ^+ in the metal, create an overall neutral effective double layer, modifying the catalyst work function and thus affecting its chemisorption properties and catalytic activity and selectivity [26–28].

When using YSZ as the solid electrolyte, the promoting ionic species ($O^{\delta-} - \delta^+$) are generated in an electrochemical step at the tpb (Eq. (9a)) which then spread, due the strong repulsive dipole–dipole interactions, over the entire metal–gas interface establishing there the neutral effective double layer,

$$O^{2-}(YSZ) \rightarrow [O^{\delta-} - \delta^+]Pt + 2e^- \quad (9a)$$

at a rate $I/2F$, where I is the current and F the Faraday's constant.

In EPOC studies under reducing conditions, as is the present case, it is likely that the promoting anionic species is a hydroxyl groups formed via:

$$O^{2-}(YSZ) + (1/2)H_2 \rightarrow [OH^{\delta-} - \delta^+] + 2e^- \quad (9b)$$

It must be clarified that the spillover species (commonly denoted $O^{\delta-} - \delta^+$ in the EPOC literature) is overall neutral as the anionic oxygen species $O^{\delta-}$ is accompanied by the image charge δ^+ in the metal. Consequently, the difference between the spillover $O^{\delta-} - \delta^+$ species, which exists only at high coverages, and normally adsorbed oxygen is only in the dipole moment (~2 vs. ~1 Debye) and not in the total charge which is zero in both cases [26].

Three parameters are commonly used to quantify the magnitude of EPOC effect, the rate enhancement ratio, ρ, defined from [26]:

$$\rho = r/r_o \quad (10)$$

where r is the electropromoted catalytic rate and r_o the open-circuit, i.e., unpromoted catalytic rate, the effective rate enhancement ratio, ρ_c, defined from [26]:

$$\rho_c = \rho/\rho_{max} \quad (11)$$

where ρ_{max} expresses the maximum allowable ρ value due to complete or, more generally, equilibrium conversion and the apparent faradaic efficiency, Λ, defined from [26]:

$$\Lambda = (r - r_o)/(I/nF) \quad (12)$$

where n is the charge of the ionic species ($n = 2$ for YSZ) and F the Faraday's constant. A reaction exhibits electrochemical promotion when $|\Lambda| > 1$, while electrocatalysis is limited to $|\Lambda| \leqslant 1$.

In a previous study on the electrochemical promotion of the water–gas shift reaction utilizing a Pd catalyst electrode deposited over a proton-conducting ceramic support (strontia–zirconia–yttria perovskite of the form $SrZr_{0.95}Y_{0.05}O_{3-a}$), it was found that H^+ pumping upon positive polarization could lead to rate enhancement, i.e., $\rho = 2$ and $\Lambda = 8$ at temperatures from 600 °C to 750 °C [29].

In the present study, the effect of electrochemical promotion of catalysis was investigated for the first time in the water–gas shift (WGS) reaction over a porous Pt catalyst electrode interfaced with YSZ at temperatures from 300 °C to 400 °C and P_{H_2O}/P_{CO} ratio values from 2.85 to 31.

2. Experimental

2.1. Sample preparation

The solid electrolyte was a closed-end tube of 8 mol% Y_2O_3-stabilized ZrO_2 (YSZ) of 13 mm outer diameter and 2 mm thickness. A platinum electrode serving as the counter and/or reference electrode was deposited on the inner side of the tube by applying a thin coating of Pt organometallic paste (Engelhard-Clal 6926), followed by calcination in air for 12 h at 800 °C. Pt was selected for the counter electrode due to its well known good performance in O_2 dissociation and electrochemical reduction.

A similar Pt catalyst electrode was deposited on the outer side of the tube, opposite to the counter electrode serving as the

working electrode. The resulting metal loading was 0.83 mg Pt/cm^2, while the geometrical area of the electrode was ~3 cm^2. The catalytically active surface area, N_G, as measured by isothermal chemical titration with O_2 adsorption, was ~1 μmol Pt [26]. The latter implies for a very small metal dispersion (<1%). The surface morphology of the solid electrolyte support and of the Pt catalyst film was examined via scanning electron microscopy (SEM). Fig. 1 presents a SEM micrograph of the Pt working-catalyst electrode surface. The morphology of Pt layer is homogeneous with significant porosity.

2.2. Catalytic activity measurements

Reactants and products analysis was performed by online gas chromatography (Varian CP2003, equipped with two TC detectors and a molecular sieve and Porapaq Q columns, for the CO, CO_2 and H_2 analysis), and IR online analyzers (EMERSON NGA2000 for the CO and CO_2 analysis). Reactants were certified standards of CO in He, which could be further diluted in He. H_2O vapor was introduced using an atmospheric pressure thermostated quartz saturator at temperatures from 5 °C to 25 °C, which allowed for vapor pressure variation between 0.8 kPa and 3.1 kPa. The atmospheric pressure fuel cell type (or double chamber) quartz reactor is shown in Fig. 2. It had a volume of ~10 cm^3 and has been previously described in detail [30]. As shown in Fig. 2, in this reactor type only the working-catalyst electrode is exposed to the reaction mixture (CO, H_2O and He), while the counter electrode is constantly exposed to ambient air. In this type of reactor, the working electrode is responsible for the observed catalytic activity, while it can be also used as an electrochemical solid-state sensor. Temperature was measured by a K-type thermocouple placed in the outer side of the quartz tube in the proximity of the working electrode. A second thermocouple placed in the inner side of the bottom of the YSZ tube (exposed in air) revealed a negligible (~3 °C) temperature difference. The gas flow and mixture composition were regulated by four mass flow controllers (Brooks). The total gas flowrate was 120 cm^3 (STP) min^{-1}, which corresponds

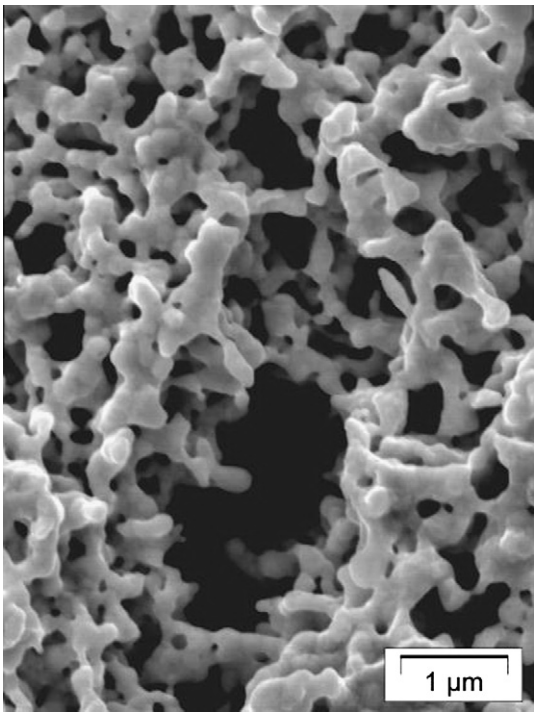

Fig. 1. SEM micrographs of the Pt catalyst electrode over the YSZ solid electrolyte support.

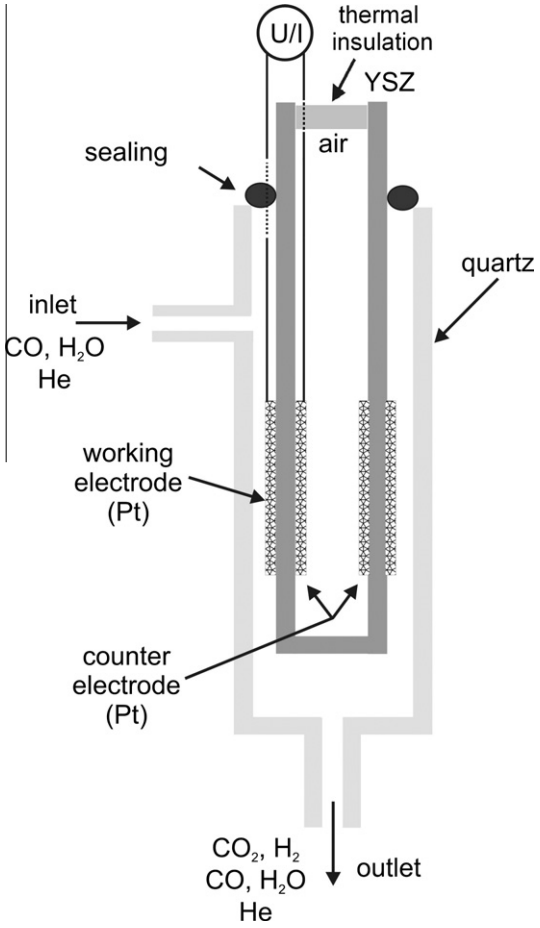

Fig. 2. Schematic of the fuel cell type electrochemical reactor.

to 5 s residence time and 1500 h^{-1} HSV (hourly space velocity) based on the reactor volume or 1300 h^{-1} WHSV (weight hourly space velocity) based on the catalyst mass (~2.5 mg). These values are comparable to the space velocities in commercial reactors under similar P_{H_2O}/P_{CO} ratio value and operation conditions. Constant currents or potentials were applied using a VoltaLab (PGP201) galvanostat–potentiostat.

3. Results and discussion

Fig. 3 shows the transient effect of constant applied negative and positive overpotential on the CO_2 formation catalytic rate, the conversion of CO and the current at 350 °C under $P_{H_2O}/P_{CO} = 31$. As shown in the figure, CO conversion was initially 42%, while negative overpotential application (η = −1.5 V) caused a pronounced increase in the reaction rate, where CO conversion reached 95%, i.e., 130% rate increase. The above value is near the thermodynamic equilibrium conversion value (~97%) at 350 °C, and thus, the effective rate enhancement ratio, ρ_c, is 0.98. This indicates that almost the maximum allowable ρ value was achieved upon negative polarization. The apparent faradaic efficiency, Λ, was −30, which shows the strong non-faradaicity and the high energy efficiency of the process.

After current interruption, the catalytic rate slowly returns to its initial value, indicating the reversibility of the phenomenon. Worth to note is that the relaxation time needed for rate recovery is much higher than the corresponding to reach the electropromoted state upon negative potential application. This is indicative of the high thickness of the Pt layer and the low operation temperature, which inhibits the thermal migration of the $O^{\delta-}$ promoting species back

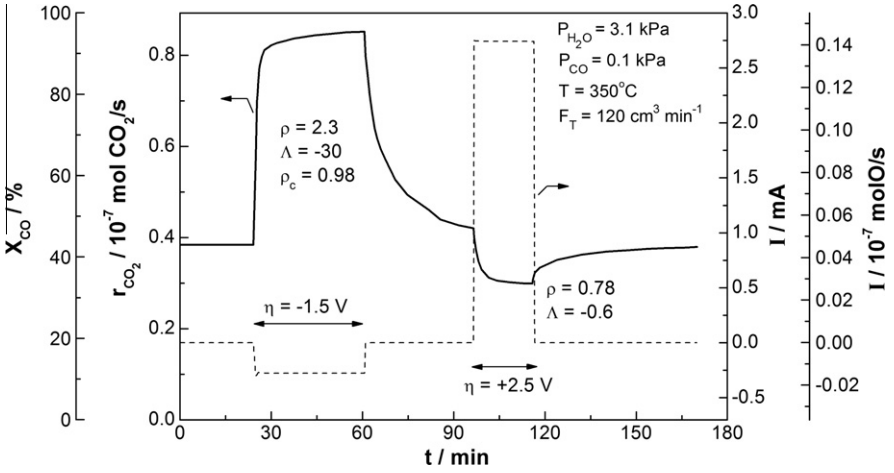

Fig. 3. Transient effect of a constant applied negative ($\eta = -1.5$ V) and positive ($\eta = +2.5$ V) overpotential on the CO_2 formation catalytic rate, the conversion of CO and the current. $T = 350$ °C.

to the catalyst surface to obtain its initial coverage. On the other hand, positive potential application, i.e., O^{2-} supply to the catalyst surface, resulted in a decrease in the CO conversion from 42% to 35%, while Λ values were lower than unity.

The observed electrophilic type behavior, i.e., rate increase upon negative polarization and rate decrease upon positive, indicates strongly adsorbed electron donor species, i.e., CO on Pt surface under open-circuit conditions. Under these conditions, there is a finite oxygen ion coverage on the Pt surface due to thermal migration of ionic species from the oxide support to the catalyst surface, which defines an open-circuit steady-state catalytic activity, by modifying the adsorbed species bond strength. Negative potential application, i.e., O^{2-} pumping from the catalyst surface, causes a decrease in the catalyst work function and thus weakening of the Pt–CO bond strength in parallel with the stabilization of the OH species (electron acceptor species) originating from water dissociation in the vicinity of Pt particles [26,27,31]. Moreover, negative potential application could also cause an increase in the surface concentration of oxygen ion vacancies, by non-stoichiometric oxygen removal at steady state, due to the lack of O_2 in the gas phase, more likely near the tpb. The latter could probably increase the WGS reaction rate due to the enhanced H_2O dissociation on oxygen vacancies (reaction (6)) in agreement with the mechanism proposed in the literature [5,7,15–18]. The enhanced H_2O dissociation and stabilization of the OH species could also facilitate the decomposition of formate intermediate species, which according to the associative mechanism [11–14,23] is rate limiting. Worth to note is that under negative polarization, the cathodic electrochemical semi-reaction taking place at the cathode, i.e., the catalyst-working electrode, is:

$$H_2O + 2e^- \rightarrow 2H + O^{2-} \quad (13)$$

On the other hand, positive potential application, i.e., O^{2-} ions supply to the catalyst surface, causes an increase in Pt work function and thus strengthening of the Pt–CO bond strength [26,27,31,32], which poisons the catalytic reaction rate. In this case, Λ values were found to be lower than unity. This can be explained on the basis of small $O^{\delta-}$ lifetime on the CO-exposed Pt surface.

Furthermore, experiments using only CO in the feed revealed a faradaic electrocatalytic oxidation of CO under positive polarization. Thus, under reaction conditions, a synergistic effect occurs between the electrocatalytic oxidation of CO and the strengthening of the Pt–CO bond strength. The latter seems to be more significant since a rate decrease is totally observed.

The observed electrophilic type behavior, i.e., rate increase by catalyst work function decrease, is in agreement with Zhai et al. [20], where the addition of K on Pt was found to result in Pt–OH_x species stabilization, which is suggested to be the active species for the low-temperature water–gas shift reaction. Similar alkali promotion has been reported by Pigos et al. [23] where Na addition was found to facilitate the formate decomposition, i.e., weakening of the C–H bond strength, which was assumed as the rate limiting.

Fig. 4 shows the effect of P_{H_2O} on the open-circuit potential (OCP) under constant P_{CO}(0.28 kPa) at 350 °C. Increase in P_{H_2O} resulted in a shift of the OCP to less negative values, indicating adsorption of electron acceptor species [25,26], i.e., hydroxyl groups (OH − s) or atomic oxygen (O − s) species, formed by water dissociation according to reactions (14) and (15), where s stands for an active site either on Pt or on YSZ.

$$H_2O(g) + s \rightarrow OH - s + 1/2H_2(g) \quad (14)$$

$$H_2O(g) + s \rightarrow O - s + H_2(g) \quad (15)$$

However, there is no evidence whether water activation occurs on Pt or YSZ or both, since OCP can be affected by adsorption on either metal particles or the support. Moreover, under open-circuit

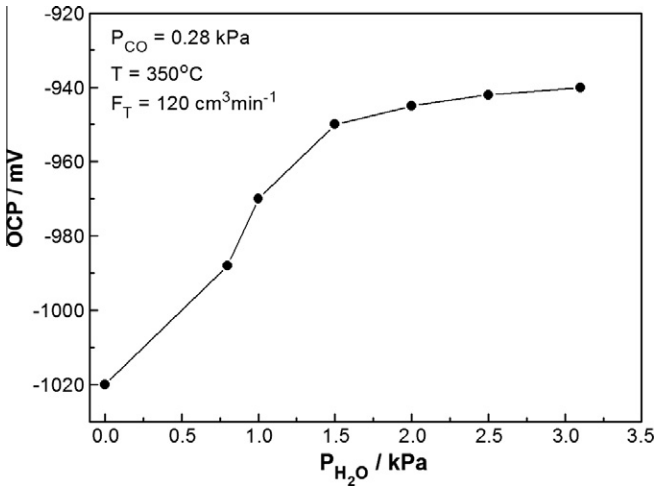

Fig. 4. Steady-state effect of the H_2O partial pressure, P_{H_2O}, on the open-circuit potential, U_{oc}, under constant volumetric gas flowrate and CO partial pressure, P_{CO}. $T = 350$ °C.

conditions, i.e., no current or potential application, the support is possible to undergo some surface reduction by CO and form oxygen vacancies necessary for water activation [17,18]. However, the possibility for reduction of the oxide support under polarization is rather limited, since all the applied cell overpotential values were kept lower than the YSZ reduction potential (~2.3 V) [26]. Worth to note is the ~100 mV change in OCP upon introduction of 3 kPa H_2O, which indicates strongly bonded CO on Pt.

The effect of the gas mixture on the OCP with respect to air at 350 °C is shown in Fig. 5. The addition of electron acceptor species, i.e., H_2O and/or O_2 in the gas phase, caused an increase in OCP, from −145 mV to −120 and −100 mV in the presence of 3.1% H_2O and 2% O_2, respectively. It is worth noting that the OCP value in the presence of O_2 reflects the different P_{O_2} values between the working (2%) and reference/counter electrode (20%). On the other hand, introduction of CO resulted in a dramatic decrease in the OCP to −1020 mV and to −940 mV in the presence of the reaction mixture (CO and H_2O). Furthermore, under 2% O_2/He where the surface concentration of oxygen vacancies near the tpb can be assumed negligible, introduction of H_2O caused ~20 mV increase in the OCP. The latter is significantly smaller than the corresponding

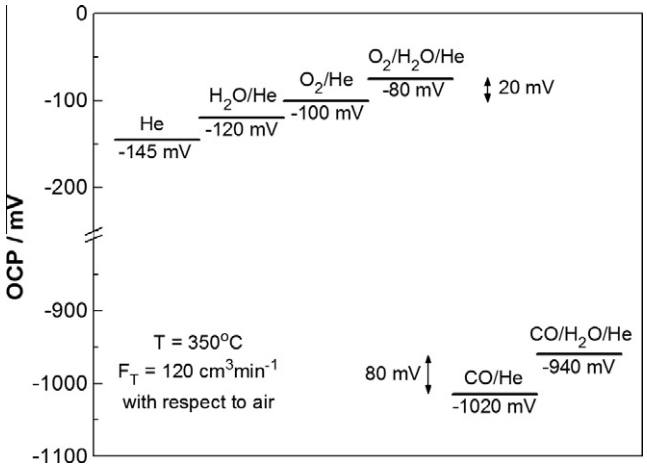

Fig. 5. The effect of gas composition on the open-circuit potential value, U_{oc}. T = 350 °C.

shift observed upon H_2O introduction under CO feed (80 mV). This difference would perhaps indicate that water adsorption and activation occur mainly on surface oxygen vacancies of the YSZ near the Pt particles. However, the effect of water dissociation on the Pt–CO bond strength and thus on the OCP has also to be considered. Another indication for water adsorption mainly on the YSZ surface (possibly on oxygen ion vacancies originating by O^{2-} backspillover onto the Pt particles) rather than on Pt could also be the higher N_G value that was calculated by isothermal chemical titration [26] with H_2O adsorption (~20 μmol Pt) than that with O_2 (~1 μmol Pt).

Fig. 6 presents a scheme of a possible electrochemical promotion mechanism for the WGS reaction, based on the proposed in literature [17,18] "associative formate with red–ox regeneration" mechanism for the case of Pt/ZrO_2. According to this mechanism, hydroxyl groups on the zirconia surface react with CO, adsorbed on Pt, to form intermediate formate. The latter decompose to H_2 and CO_2, leaving oxygen vacancies that are filled by hydroxyl groups (reactions (6) and (7)). As mentioned before, surface oxygen ion vacancies can be created due to O^{2-} thermal migration and backspillover onto the Pt surface, but also by partial reduction of the oxide support in the presence of CO. As shown in the scheme, negative polarization can lead to weakening of the Pt–CO bond strength [26] but also to an increase in surface concentration of oxygen vacancies near the tpb at steady state, which facilitates the [OH] species adsorption. On the other hand, positive polarization (not shown here) causes an increase in the Pt–CO bond strength, which poisons the catalytic activity and results in rate decrease.

The steady-state effect of P_{CO} on the conversion of CO and CO_2 formation rate and turnover frequency (TOF) under open-circuit and positive and negative polarization conditions at 350 °C under constant gas flowrate is presented in Fig. 7a. Under open-circuit conditions, a negative effect of P_{CO} on the CO_2 formation rate was observed, where it decreased from 0.4×10^{-7} mol CO_2 s^{-1} at 0.1 kPa CO to 0.3×10^{-7} mol CO_2 s^{-1} at 0.37 kPa CO. This negative effect indicates the strong adsorption bond strength of CO on Pt. The latter agrees with the electrophilic type behavior that observed in Fig. 3 [26,31]. Positive potential application (η = +2.5 V) resulted in a rate decrease in the examined P_{CO} range with a similar negative effect of P_{CO}. On the contrary, negative potential application (η = −1.5 V) caused a significant increase in the catalytic rate,

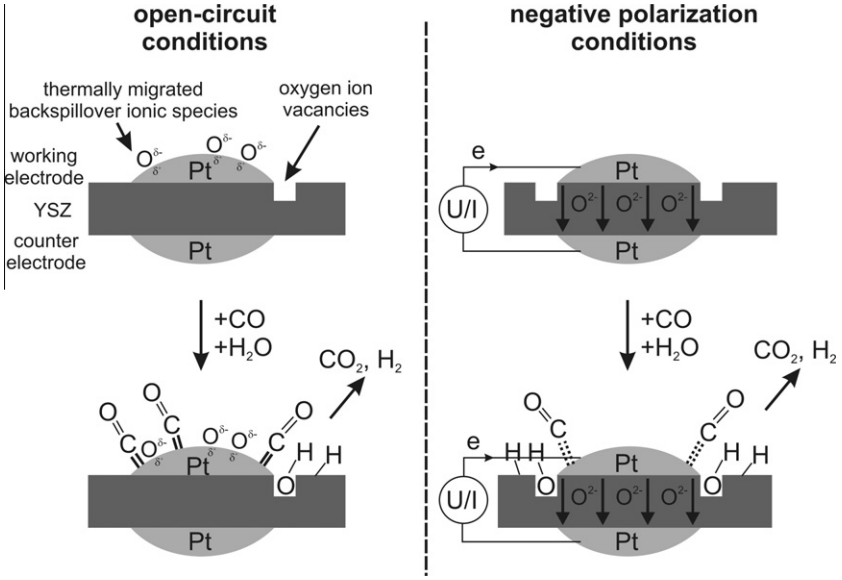

Fig. 6. Schematic of a possible electrochemical promotion mechanism for the WGS reaction.

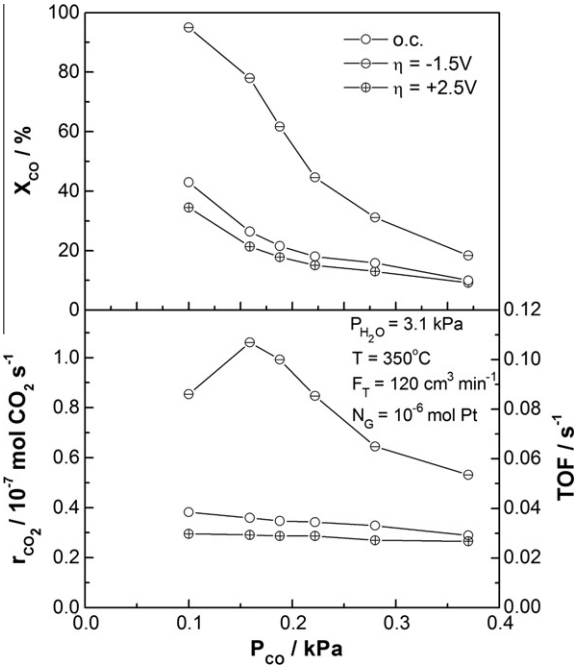

Fig. 7a. Steady-state effect of the CO partial pressure, P_{CO}, on the CO_2 formation rate and the conversion of CO, under constant volumetric gas flowrate and H_2O partial pressure, P_{H_2O}. $T = 350$ °C.

where the negative effect of P_{CO} on the reaction rate was more pronounced than that under open-circuit conditions. The observed maximum in the reaction rate under negative potential application could be attributed to an optimal CO coverage over the catalyst. Turnover frequency, TOF, values $\sim 0.03\ s^{-1}$ were found under open-circuit conditions, while negative potential application caused a TOF increase up to $0.11\ s^{-1}$. These values, which were calculated using $N_G = 10^{-6}$ mol Pt, are close to those reported in literature and fall between 0.5 and $1\ s^{-1}$ [9,21,33] at 350 °C depending on the P_{H_2O}/P_{CO} ratio.

The steady-state effect of P_{H_2O} on the conversion of CO and CO_2 formation rate under open-circuit and positive and negative polarization conditions is shown in Fig. 7b, at 350 °C under constant gas flowrate. Under open-circuit conditions, a positive effect of P_{H_2O} on the CO_2 formation rate was observed, where the conversion of CO increased from 19% at 0.8 kPa H_2O to 29% at 3.1 kPa CO. The positive effect of P_{H_2O} on the rate indicates the weak adsorption bond strength of electron acceptor species, i.e., hydroxyl groups. This result is in agreement with the electrophilic type behavior, which is observed under strongly adsorbed electron donor species and weakly adsorbed electron acceptor species [26,31]. A similar positive effect of P_{H_2O} was observed both under positive and negative potential application ($\eta = +2.5$ V).

Fig. 8 shows the steady-state effect of P_{CO} on the rate enhancement ratio, ρ, and the apparent faradaic efficiency, Λ, values under 3.1 kPa P_{H_2O}. As shown, ρ and Λ values up to 3 and −50, respectively, were obtained at low P_{CO} values and under negative potential application, while the magnitude of EPOC effect decreased by increase of P_{CO} or decrease of the P_{H_2O}/P_{CO} ratio. On the other hand, smaller ρ values were obtained upon positive polarization, where the effect was sub-faradaic, i.e., $|\Lambda| < 1$ [34,35].

Fig. 9 shows the steady-state effect of the applied potential (U) and overpotential (η) on the rate enhancement ratio, ρ, and the apparent faradaic efficiency, Λ, values at 3.1 kPa P_{H_2O} and 0.28 kPa P_{CO} at 350 °C. As shown, a maximum ρ value was observed at the optimum overpotential value $\eta = -1.5$ V, probably due to an optimal catalyst work function value and thus an optimal reactants' coverage (more likely CO) of the catalyst electrode, in agreement with Fig. 7a. Similar optimal applied potential values have been reported in previous EPOC studies under positive polarization and were attributed to site blocking effects by backspillover $O^{\delta-}$ promoting ions on the positively polarized catalyst electrode [34,35].

Arrhenius plots of the unpromoted and electropromoted reaction rate of the WGS reaction are shown in Fig. 10. Negative potential application caused a pronounced increase in the apparent activation energy, E_a, from 6 to 10.5 kcal mol^{-1}, while positive polarization led to a small decrease to 5 kcal mol^{-1}. These values are close to those reported for this reaction in literature, which fall between 7.2 and 11 kcal mol^{-1} [6,16,36,37]. The observed increase in E_a upon negative polarization and rate increase could be attributed either to a gradual change in the rate-limiting step under negative polarization conditions or to the fact that negative polarization can be more effective at lower temperatures. The latter could be rationalized in the basis of weak CO adsorption on Pt

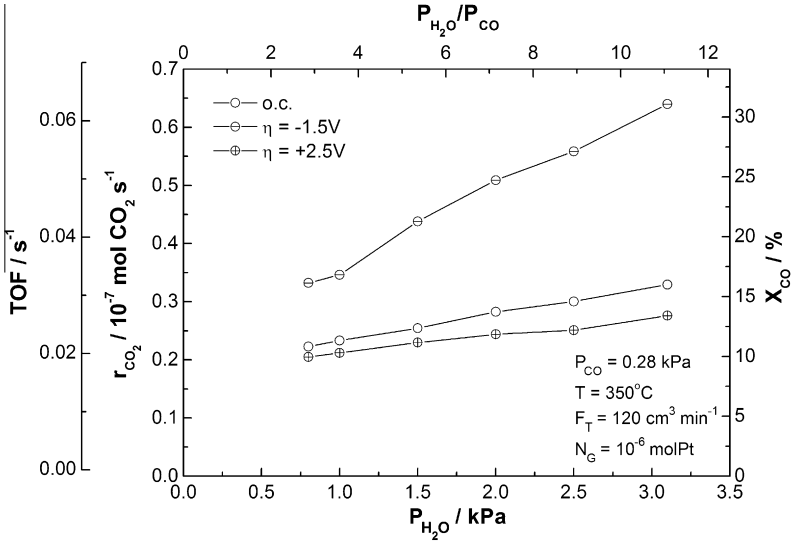

Fig. 7b. Steady-state effect of the H_2O partial pressure, P_{H_2O}, on the CO_2 formation rate and the conversion of CO, under constant volumetric gas flowrate and CO partial pressure, P_{CO}. $T = 350$ °C.

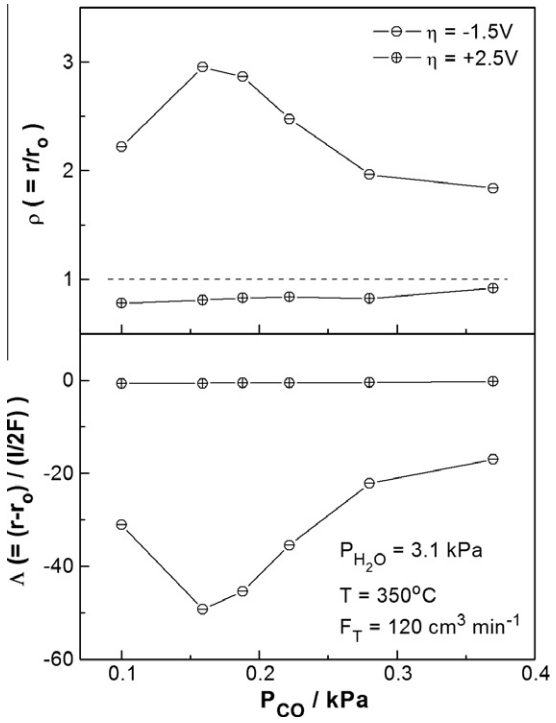

Fig. 8. Steady-state effect of CO partial pressure, P_{CO}, on the apparent faradaic efficiency, Λ, and the rate enhancement ratio, ρ, under both positive and negative potential application. T = 350 °C.

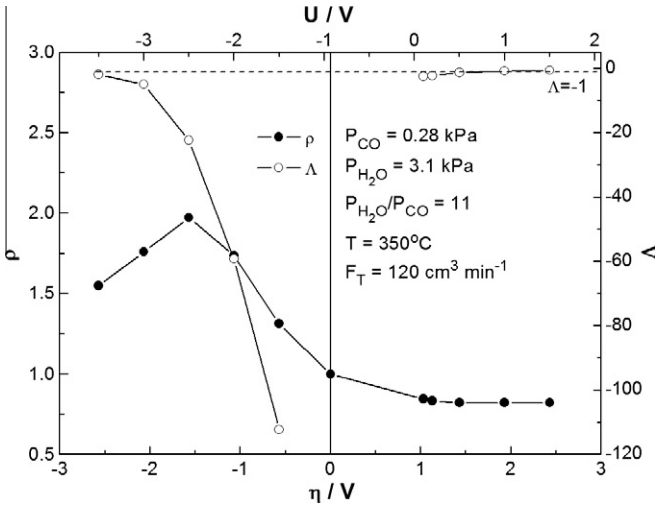

Fig. 9. Steady-state effect of the applied overpotential on the rate enhancement ratio, ρ, and the apparent faradaic efficiency, Λ, under P_{H_2O} = 3.1 kPa and P_{CO} = 0.28 kPa, T = 350 °C.

at high temperatures and thus smaller effect of $O^{\delta-}$ pumping under negative polarization.

A linear dependence of the apparent activation energy on the catalyst work function, $\Delta\Phi$, has been observed and reported also in previous EPOC studies [26] and conforms to the equation [9,21,33]:

$$E_a = E_a^{oc} + a_H \Delta\Phi \quad (16)$$

where E_a^{oc} is the apparent activation energy in the unpromoted state (6 kcal mol^{-1}) and a_H is a constant, which is usually negative. In this case, a_H was calculated ~−1.3.

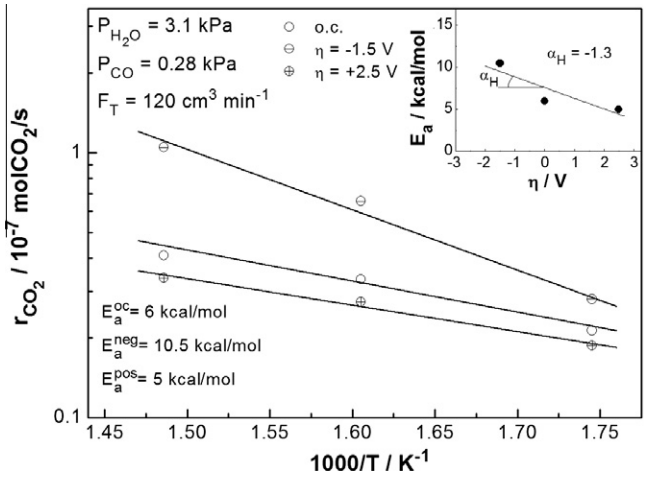

Fig. 10. Arrhenius plots under open-circuit (oc) state and negative (−1.5 V) and positive (+2.5 V) overpotential application conditions. Inset: effect of overpotential on the apparent activation energy, E_a.

Eq. (16) can also be written in the form:

$$E_a = E_a^{oc} + a_H e \Delta U \quad (17)$$

since the work function change, $\Delta\Phi$, is related to the change in catalyst potential, ΔU, via [26,27]:

$$\Delta\Phi = e\Delta U \quad (18)$$

where e is the electron charge.

3.1. Kinetic measurements

The effect of partial pressure of reactants (CO, H_2O) on the kinetic rate of the WGS reaction was investigated at 350 °C. Fig. 11a shows the dependence of the intrinsic reaction rate on the partial pressure of CO, where H_2O partial pressure was kept constant at 3.1 kPa. The total gas flowrate kept high in order to obtain differential conditions, i.e., less than 10% conversion. As shown, the increase in CO partial pressure led to a slight decrease in the WGS reaction rate under either open-circuit state or negative polarization conditions, similar to Fig. 7a. On the other hand, one observes a positive effect of P_{H_2O} on the intrinsic rate under

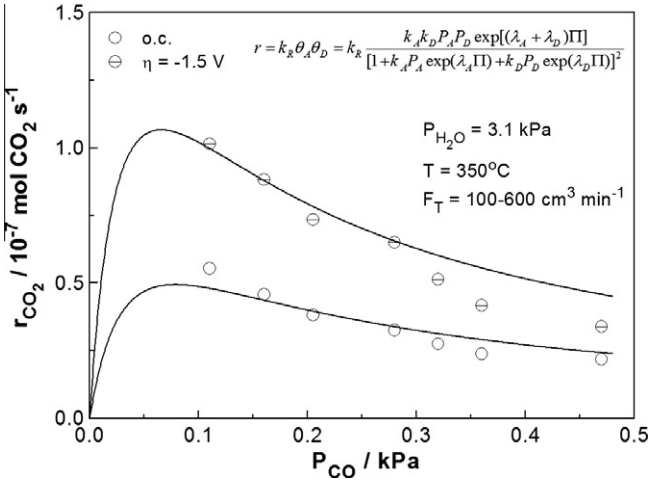

Fig. 11a. Steady-state effect of the CO partial pressure, P_{CO}, on the kinetic CO_2 formation rate under constant H_2O partial pressure, P_{H_2O}. $(\ell/2d)\cos\omega$ = 1, F_T = 100–600 cm^3 min^{-1}, T = 350 °C.

both open-circuit state and negative potential application conditions (Fig. 11b). The reaction rate order value with respect to CO partial pressure P_{CO}, reported in literature of Pt-based catalysts, varies between −1 and 1, while positive (near 1) is the order with respect to P_{H_2O} [8,29,36,38–40].

The effective double-layer (EDL) isotherm Eq. (18), as has been developed by Brosda and Vayenas [41] for adsorption in the presence of the "effective double layer", has been used to fit the experimental intrinsic rate data shown in Figs. 11a and 11b, using FORTRAN programming environment. The points shown in the figures correspond to the experimental data, while the solid curve to the theoretically predicted rate according to the EDL model, i.e.:

$$\theta_j/(1-\theta_j) = k_j P_j \exp(-\lambda_j \Pi) \tag{19}$$

where θ_j is the coverage of the adsorbed j, k_j is the adsorption coefficient which quantifies the chemisorptive bond strength of j at the potential of zero charge of the double layer, P_j is the partial pressure of j in the gas phase, λ_j is the partial charge transfer parameter of the adsorbed j which is directly related to the dipole moment of the adsorbed j ($\lambda > 0$ for the electron donor species and $\lambda < 0$ for the electron acceptor species), and Π is the dimensionless potential defined by Eq. (20a) [41].

$$\Pi = \Delta\Phi\left(\frac{\ell}{2d}\cos\omega\right)/k_b T \tag{20a}$$

where ℓ is the distance between the centers of the positive and negative charges in the adsorbed dipole, d is the thickness of the homogeneous double layer, $\Delta\Phi$ (=$\Phi - \Phi_0$) is the work function difference between that of the actual surface and that of the surface at its potential of zero charge [26,31,41–43], where the field strength in the double layer vanishes and $\Phi = \Phi_0$, ω is the angle formed between the adsorbate dipole and the field, which is vertical to the catalyst electrode, and k_b the Boltzmann's constant. In this analysis, we assume adsorption in the direction of the field, thus $\omega = 0^o$ and also that $\ell \approx 2d$. Hence, Eq. (20a) can also be written, using Eq. (18), in the form:

$$\Pi \approx e\Delta U/k_b T \tag{20b}$$

This model, which can be viewed as an extension of Langmuir–Hinshelwood–Hougen–Watson kinetics, is based on electrochemical

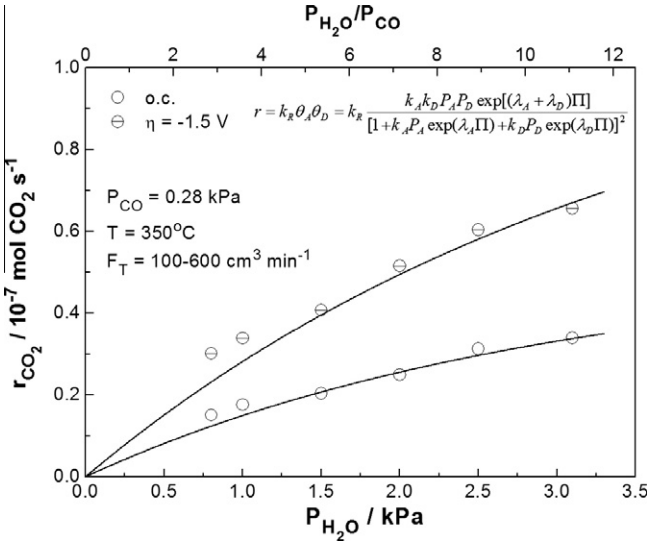

Fig. 11b. Steady-state effect of the H_2O partial pressure, P_{H_2O}, on the intrinsic CO_2 formation rate under constant CO partial pressure, P_{H_2O}. $(\ell/2d)\cos\omega = 1$, $F_T = 100$–$600\ cm^3\ min^{-1}$, $T = 350\ ^\circ C$.

Table 1
Effect of negative polarization on the parameters of the effective double-layer (EDL) isotherm kinetic model.

Model parameters	Open-circuit conditions OCP = −0.94 V $\eta = 0$ $\Pi = -17.52$	Negative polarization $U = -2.44$ V $\eta = -1.5$ V $\Pi = -46.56$
k_R	2×10^{-7}	4.5×10^{-7}
k_A	3	10
k_D	1000	500
λ_A	−0.12	−0.0008
λ_D	0.001	0.0001
k_R^0	1.2×10^{-7}	

Langmuir-type adsorption isotherms that are mathematically similar to Frumkin isotherms [41] and can account explicitly for the attractive or repulsive electrostatic interactions between the adsorbates and the "effective double layer" present at the catalyst–gas interface [41]. Here, we make the assumption for competitive adsorption of H_2O and CO on the same active sites.

Using Eq. (19), the catalytic rate can be expressed as:

$$r = k_R\theta_A\theta_D = k_R\frac{k_A k_D P_A P_D \exp[(\lambda_A+\lambda_D)\Pi]}{[1+k_A P_A \exp(\lambda_A\Pi)+k_D P_D \exp(\lambda_D\Pi)]^2} \tag{21}$$

where k_R is the surface reaction rate constant which can in general be expressed by:

$$k_R = k_R^o \exp\left(\frac{aF}{RT}U\right) \tag{22}$$

where k_R^0 is the rate constant at zero potential conditions ($U = 0$ V) and α the transfer coefficient, which is related to λ_A and λ_D.

Table 1 summarizes the values of the parameters of the model (k_R, k_A, k_D, λ_A, λ_D and k_R^0) in open-circuit state and under negative and positive polarization conditions at 350 °C. No results under positive potential application are presented here since the effect was faradaic and no EPOC was observed. As shown, the surface reaction rate constant, k_R, increases by potential decrease (negative polarization) in agreement with Eq. (22), since $\alpha < 0$ for electrophilic type behavior. Worth noting is the almost three orders of magnitude difference between k_A and k_D, which indicates the strong CO adsorption bond strength on Pt. Moreover, an increase in k_A and an even more pronounced decrease in k_D were observed by negative polarization, indicating the weakening of the electron donor species, i.e., CO, bond strength on the catalyst surface and the strengthening of the electron acceptor species, i.e., OH, by negative potential application. This agrees with the observed electrophilic type behavior.

4. Conclusions

The effect of electrochemical promotion of catalysis on the water–gas shift reaction was investigated over porous Pt catalyst electrodes interfaced with YSZ, in a fuel cell type electrochemical reactor at temperatures from 300 °C to 400 °C, under P_{H_2O}/P_{CO} ratio values from 2.85 to 31. A negative-order dependence of the catalytic reaction rate on P_{CO} and a positive on P_{H_2O} was found under open-circuit and under polarization conditions.

Positive overpotential application ($\eta = +2.5$ V), i.e., O^{2-} supply to the catalyst surface, causes a small decrease in the catalytic reaction rate, while negative potential application ($\eta = -1.5$ V) results in a pronounced rate increase, up to 200%, with apparent faradaic efficiency values up to 110 (under $\eta = -0.5$ V). The observed rate increase upon negative polarization can be mainly attributed to the weakening of the Pt–CO bond strength but also, to the increase in surface concentration of oxygen ion vacancies, by

removing non-stoichiometric oxygen from YSZ, near the Pt-gas-support three-phase boundaries that are necessary for water dissociation.

References

[1] D.S. Newsome, Catal. Rev. Sci. Eng. 21 (1980) 275.
[2] K.-O. Hinrichsen, K. Kochloefl, M. Muhler, in: G. Ertl, H. Knozinger, J. Weitkamp (Eds.), Handbook of Heterogeneous Catalysis, second ed., VCH, Ludwigshafen, 2008. pp. 2905–2920.
[3] A.R. de la Osa, A. De Lucas, J.L. Valverde, A. Romero, I. Monteagudo, P. Sánchez, Int. J. Hydrogen Energy 36 (2011) 44–51.
[4] M.A. Henderson, Surf. Sci. Rep. 46 (2002) 1–308.
[5] K. Takanabe, K.-i. Aika, K. Seshan, L. Lefferts, J. Catal. 227 (2004) 101–108.
[6] T. Bunluesin, R.J. Gorte, G.W. Graham, Appl. Catal. B 15 (1998) 107–114.
[7] R.J. Gorte, S. Zhao, Catal. Today 104 (2005) 18–24.
[8] D.C. Grenoble, M.M. Estadt, D.F. Ollis, J. Catal. 67 (1981) 90–102.
[9] P. Panagiotopoulou, D.I. Kondarides, Catal. Today 112 (2006) 49–52.
[10] G. Jacobs, S. Ricote, B.H. Davis, Appl. Catal. A 302 (2006) 14–21.
[11] G. Jacobs, U.M. Graham, E. Chenu, P.M. Patterson, A. Dozier, B.H. Davis, J. Catal. 229 (2005) 499–512.
[12] A. Goguet, S.O. Shekhtman, R. Burch, C. Hardacre, F.C. Meunier, G.S. Yablonsky, J. Catal. 237 (2006) 102–110.
[13] S.Y. Choung, M. Ferrandon, T. Krause, Catal. Today 99 (2005) 257–262.
[14] G. Jacobs, E. Chenu, P.M. Patterson, L. Williams, D. Sparks, G. Thomas, B.H. Davis, Appl. Catal. A 258 (2004) 203–214.
[15] X. Wang, R.J. Gorte, Appl. Catal. A 247 (2003) 157–162.
[16] S. Hilaire, X. Wang, T. Luo, R.J. Gorte, J. Wagner, Appl. Catal. A 215 (2001) 271–278.
[17] K.G. Azzam, I.V. Babich, K. Seshan, L. Lefferts, J. Catal. 251 (2007) 153–162.
[18] P.O. Graf, D.J.M. de Vlieger, B.L. Mojet, L. Lefferts, J. Catal. 262 (2009) 181–187.
[19] S.T. Korhonen, M. Calatayud, A.O.I. Krause, J. Phys. Chem. C 112 (2008) 16096–16102.
[20] Y. Zhai, D. Pierre, R. Si, W. Deng, P. Ferrin, A.U. Nilekar, G. Peng, J.A. Herron, D.C. Bell, H. Saltsburg, M. Mavrikakis, M. Flytzani-Stephanopoulos, Science 329 (2010) 1633–1636.
[21] P. Panagiotopoulou, D.I. Kondarides, J. Catal. 267 (2009) 57–66.
[22] P. Panagiotopoulou, D.I. Kondarides, Appl. Catal. B 101 (2011) 738–746.
[23] J.M. Pigos, C.J. Brooks, G. Jacobs, B.H. Davis, Appl. Catal. A 328 (2007) 14–26.
[24] J.M. Pigos, C.J. Brooks, G. Jacobs, B.H. Davis, Appl. Catal. A 319 (2007) 47–57.
[25] C. Wagner, Adv. Catal. 21 (1970) 323–381.
[26] C.G. Vayenas, S. Bebelis, C. Pliangos, S. Brosda, D. Tsiplakides, Electrochemical Activation of Catalysis: Promotion, Electrochemical Promotion, and Metal-Support Interactions, Kluver Academic/Plenum Publishers, New York, 2001. 574.
[27] C.G. Vayenas, C.G. Koutsodontis, J. Chem. Phys. 128 (2008) 182506.
[28] A. Katsaounis, J. Appl. Electrochem. 40 (2010) 885–902.
[29] C. Kokkofitis, M. Ouzounidou, A. Skodra, M. Stoukides, Solid State Ionics 178 (2007) 475–480.
[30] X. Li, F. Gaillard, P. Vernoux, Top. Catal. 44 (2007) 391–398.
[31] C.G. Vayenas, S. Brosda, C. Pliangos, J. Catal. 203 (2001) 329–350.
[32] L. Lizarraga, S. Souentie, L. Mazri, A. Billard, P. Vernoux, Electrochem. Commun. 12 (2010) 1310–1313.
[33] Q. Fu, W. Deng, H. Saltsburg, M. Flytzani-Stephanopoulos, Appl. Catal. B 56 (2005) 57–68.
[34] S. Souentie, A. Hammad, S. Brosda, G. Foti, C.G. Vayenas, J. Appl. Electrochem. 38 (2008) 1159–1170.
[35] A. Hammad, S. Souentie, E.I. Papaioannou, S. Balomenou, D. Tsiplakides, J.C. Figueroa, C. Cavalca, C.J. Pereira, Appl. Catal. B 103 (2011) 336–342.
[36] C.M. Kalamaras, P. Panagiotopoulou, D.I. Kondarides, A.M. Efstathiou, J. Catal. 264 (2009) 117–129.
[37] K.G. Azzam, I.V. Babich, K. Seshan, L. Leffers, Appl. Catal. B 80 (2008) 129.
[38] A.B. Mhadeshwar, D.G. Vlachos, Catal. Today 105 (2005) 162–172.
[39] A.A. Phatak, N. Koryabkina, S. Rai, J.L. Ratts, W. Ruettinger, R.J. Farrauto, G.E. Blau, W.N. Delgass, F.H. Ribeiro, Catal. Today 123 (2007) 224–234.
[40] R. Radhakrishnan, R.R. Willigan, Z. Dardas, T.H. Vanderspurt, Appl. Catal. B 66 (2006) 23–28.
[41] S. Brosda, C.G. Vayenas, J. Catal. 208 (2002) 38–53.
[42] D. Tsiplakides, C.G. Vayenas, J. Electrochem. Soc. 148 (2001) E189–E202.
[43] C.G. Vayenas, S. Brosda, C. Pliangos, J. Catal. 216 (2003) 487–504.